CAMBRIDGE
UNIVERSITY PRESS

RESEARCH ARTICLE

Optimal design of a new redundant spherical parallel manipulator with an unlimited self-rotation capability

Chaima Lahdiri[1], Houssem Saafi[1,2] , Abdelfattah Mlika[1] and Med Amine Laribi[3]

[1]Mechanical Laboratory of Sousse, University of Sousse, Sousse, Tunisia.
[2]Preparatory institute for engineering studies of Gafsa, University of Gafsa, Gafsa, Tunisia.
[3]Department of GMSC, Pprime Institute, CNRS– University of Poitiers, ENSMA– UPR 3346, Poitiers, France
Corresponding author: Houssem Saafi; Email: houssem.saafi@gmail.com

Abstract

This paper deals with the optimization of a new redundant spherical parallel manipulator (New SPM). This manipulator consists of two spherical five-bar mechanisms connected by the end-effector, providing three degrees of freedom, and has an unlimited self-rotation capability. Three optimization procedures based on the genetic algorithm method were carried out to improve the dexterity of the New SPM. The first and the second optimizations were applied to a symmetric New SPM structure, while the third was applied to an asymmetric New SPM structure. In both cases, the optimization was performed using an objective function defined by the quadratic sum of link angles. In addition, certain criteria and constraints were implemented. The obtained results demonstrate significant improvements in the dexterity of the New SPM and its capability of an unlimited self-rotate in an extended workspace. A comparison of the self-rotation performances between the classical 3-RRR SPM (R for revolute joint) and the New SPM is also presented.

1. Introduction

Teleoperation systems play a crucial role in medical robotics, as they enable surgeons to control robotic instruments dedicated to medical applications. These teleoperation systems typically consist of two stations: a slave station and a master station, connected by a control unit. The surgeons manipulate the slave robots by using haptic devices placed in the master station. The haptic device captures gestures and movements and then converts them into commands that are subsequently sent to the slave robots.

Minimally invasive surgery (MIS) is a surgical technique that involves making small incisions in the body and inserting thin instruments and a camera to perform the operation. One example of a teleoperation system for MIS is the da Vinci Surgical System, which consists of a master console where the surgeon sits and manipulates two hand controllers and a slave robot that has four arms with various surgical tools and a camera. The movement of the surgical tool is defined by three rotations and one translation, which correspond to the roll, pitch, yaw, and the insertion of the tool. The prescribed workspace for the tool is a cone with an apex angle of 26° [1].

Several researches have focused on the development of haptic devices [2, 3]. Many of them have been created for medical applications. One such haptic device is the PHANTOM OMNI [4]. It is frequently used in surgical training and simulation. It provides six degrees of freedom and has a serial structure; its force feedback allows three forces and three torques on a wrist. The Virtuose [5] is a serial haptic device used in medical training for MIS providing force sensing. It is also applied in rehabilitation and teleoperation. A spherical parallel manipulator (SPM) has been developed by Chaker et al. [1] as a haptic

device. It provides three rotations around a fixed point, and it is integrated into a robotic system designed to assist surgeons during minimally invasive procedures. In ref. [6], Najafi et al. have developed a haptic device for remote ultrasound imaging, which has a hybrid architecture with four degrees of freedom: three rotations and one translation. All the haptic devices previously cited have different structures: parallel, serial, and hybrid. The serial structure has the advantage of a simple kinematic, direct control models, and a large workspace. However, it has a lower stiffness and lower rigidity compared to the parallel structure.

SPMs are a class of parallel robots that offer three degrees of freedom of rotation. SPMs are frequently used as haptic devices. For instance, a haptic device called "Shade" [7] was developed to allow a human operator to control the orientation of a distant "camera" while receiving force feedback. A new type of spherical parallel haptic device [8] using electrorheological fluid has been developed for MIS applications. It can track well both torque and force, which are required for surgical operations.

However, SPMs present some problems, such as parallel singularities inside their workspace [9], limited self-rotation capabilities [10], and a reduced workspace [9, 10]. To solve the problem of parallel singularities, various methods have been proposed based on: geometric optimization [11–13] or redundancy [14–20]. For instance, Saafi et al. [21, 22] succeeded in eliminating singularities by proposing a redundant spherical SPM. Despite these various solutions, the problem of limited self-rotation remains unsolved. Achieving extended self-rotation is crucial for different medical procedures, including MIS, neurosurgery, tele-echography, and medical education.

A 3-RRR spherical parallel manipulator with coaxial input axes (SPM coaxial) has been developed with infinite self-rotation capabilities [23]. This manipulator is made of three legs sharing a common input axis of rotation. Despite the infinite rotation capability of the coaxial SPM, it presents several disadvantages: firstly, integrating direct drive motors proves challenging due to the shared axis of rotation. Additionally, the placement of absolute sensors is a complex task. The sensors are crucial for the implementation of feedback mechanisms for precise control. Moreover, to achieve a full rotation, the entire structure must fully rotate, introducing inertia-related issues that can affect the stability and control of the manipulator. For our proposed mechanism, each actuator and sensor are placed in a different axis with different direction. This facilitates the actuators and sensors equipment. In addition, to achieve a full rotation, only the moving platform performs a full rotation.

In this work, we propose a new redundant SPM (New SPM) with unlimited self-rotation capabilities. The New SPM is composed of two spherical five-bar mechanisms connected by the mobile platform. To achieve a unlimited rotation, only the moving platform performs a full rotation. Additionally, the kinematic models of this structure are less complex than the classical spherical parallel manipulator since the structure is composed of two simple spherical five-bar mechanisms. The redundant structure has allowed having a large free-singular useful workspace. An optimization based on the genetic algorithm is carried out to identify the optimal design parameters. In addition, we have studied the self-rotation capability within the workspace, proving its enhancement over the classic SPM.

This paper is organized as follows: In Section 2, the new kinematic of the spherical parallel robot is detailed. Section 3 presents the distribution of the dexterity of the New SPM. In Section 4, we discuss optimization methods and then compare the self-rotation performance of the classical SPM and the New SPM. The last section is dedicated to the conclusions and additional perspectives concerning this work.

2. The new spherical parallel manipulator structure

The New SPM has a spherical parallel architecture with three rotational degrees of freedom: two tilt rotations, and one self-rotation. The New SPM is made of two five-bar mechanisms connected by the mobile platform as shown in Fig. 1. The first five-bar mechanism is defined by the two legs A and B, and the second is defined by the legs C and D. Each five-bar mechanism is composed of four links and five revolute joints. All axes of the revolute joints intersect in the center of rotation (CoR). The four revolute joints linked to the base are actuated. These actuators will generate the force feedback to the
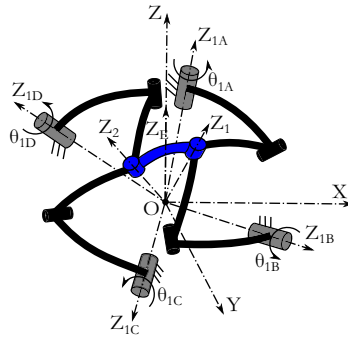
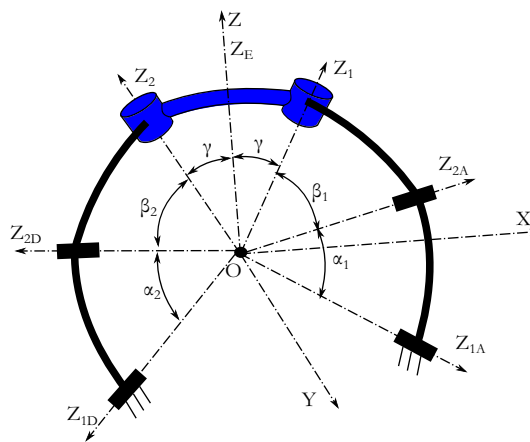**Figure 1.** *New redundant spherical parallel manipulator kinematic.*

Figure 2. *Parameters of legs A and D.*

manipulator. Since the number of actuators is greater than the degrees of freedom, the New SPM is defined as a redundant structure.

The size of each link is defined by the angle between its two revolute joints and its radius (see Fig. 2). The dimensions of the proximal links, connected to the base, and the distal links, connected to the mobile platform, are denoted by angles α_j and β_j, respectively ($j = 1$ for legs A and B and $j = 2$ for legs C and D). The orientation of the axis Z_{1k} with respect to the Z-axis is defined by the angles δ. The orientation of the mobile platform is described by the ZXZ Euler angles ψ, θ, and φ.

3. Kinematic behavior of the New SPM

The inverse kinematic model of the New SPM is expressed by Eq. (1):

$$\begin{cases} \mathbf{Z}_{2K} \cdot \mathbf{Z}_1 = \cos \beta_1 \ , \ K = A, B \\ \mathbf{Z}_{2K} \cdot \mathbf{Z}_2 = \cos \beta_2 \ , \ K = C, D \end{cases} \tag{1}$$

With,

$\mathbf{Z}_{2k} = \mathbf{Rot}(\mathbf{Z}, i \times \dfrac{\pi}{4}) \cdot \mathbf{Rot}(\mathbf{X}, \delta) \cdot \mathbf{Rot}(\mathbf{Z}_{1k}, \theta_{1k}) \cdot \mathbf{Rot}(X_{1k}, \alpha_j) \cdot \mathbf{Z}$, for $\ \ i = 1, 3, 5, 7$

and,

$\mathbf{Z}_1 = \mathbf{Rot}(\mathbf{Z}, \psi) \cdot \mathbf{Rot}(\mathbf{X}, \theta) \cdot \mathbf{Rot}(\mathbf{Z}, \varphi) \cdot \mathbf{Rot}(\mathbf{Y}, -\gamma) \cdot \mathbf{Z}$

$\mathbf{Z}_2 = \mathbf{Rot}(\mathbf{Z}, \psi) \cdot \mathbf{Rot}(\mathbf{X}, \theta) \cdot \mathbf{Rot}(\mathbf{Z}, \varphi) \cdot \mathbf{Rot}(\mathbf{Y}, \gamma) \cdot \mathbf{Z}$
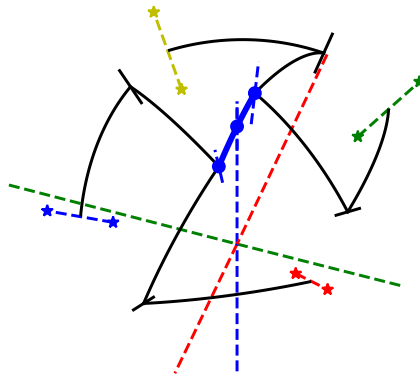
Figure 3. *The best dexterity's working mode of the New SPM.*

After developing and rearranging Eq. (1), we get the following Eq. (2):

$$A_i \cos \theta_{1k} + B_i \sin \theta_{1k} + C_i = 0, \quad i = 1, 2, 3, 4 \tag{2}$$

Where A_i, B_i, and C_i ($i = 1, 2, 3, 4$) are variables that depend on the geometric parameters (α, β, δ, γ) and the Euler angles (ψ, θ, and φ).

The inverse kinematic model of the New SPM has sixteen possible solutions, obtained by combining the solutions of the angles (θ_{1A}, θ_{1B}, θ_{1C}, θ_{1D}). These solutions present the working mode of the manipulator. In a previous work [24], we demonstrated that the working mode shown in Fig. 3 has the best dexterity distribution and less interference between the links. Therefore, this working mode has been selected.

The kinematic model can be obtained by differentiating Eq. (1) as a function of time. The obtained equation can be written as follows:

$$\begin{cases} \dot{\mathbf{Z}}_{2K} \cdot \mathbf{Z}_1 + \mathbf{Z}_{2K} \cdot \dot{\mathbf{Z}}_1 = 0 \,, K = A, B \\ \dot{\mathbf{Z}}_{2K} \cdot \mathbf{Z}_2 + \mathbf{Z}_{2K} \cdot \dot{\mathbf{Z}}_1 = 0 \,, K = C, D \end{cases} \tag{3}$$

with, $\quad \begin{cases} \dot{\mathbf{Z}}_{2K} = \dot{\theta}_{1k} \cdot \mathbf{Z}_{1K} \times \mathbf{Z}_{2K} \\ \dot{\mathbf{Z}}_1 \;\; = \Omega \times \mathbf{Z}_1 \\ \dot{\mathbf{Z}}_2 \;\; = \Omega \times \mathbf{Z}_2 \end{cases}$

Where Ω is the angular velocity of the moving platform. The equations for the four legs are illustrated as follows:

$$\begin{cases} \mathbf{Z}_{1A} \times \mathbf{Z}_{2A} \cdot \mathbf{Z}_1 \cdot \dot{\theta}_{1A} = \mathbf{Z}_{2A} \times \mathbf{Z}_1 \cdot \Omega \\ \mathbf{Z}_{1B} \times \mathbf{Z}_{2B} \cdot \mathbf{Z}_1 \cdot \dot{\theta}_{1B} = \mathbf{Z}_{2B} \times \mathbf{Z}_1 \cdot \Omega \\ \mathbf{Z}_{1C} \times \mathbf{Z}_{2C} \cdot \mathbf{Z}_2 \cdot \dot{\theta}_{1C} = \mathbf{Z}_{2C} \times \mathbf{Z}_2 \cdot \Omega \\ \mathbf{Z}_{1D} \times \mathbf{Z}_{2D} \cdot \mathbf{Z}_2 \cdot \dot{\theta}_{1D} = \mathbf{Z}_{2D} \times \mathbf{Z}_2 \cdot \Omega \end{cases} \tag{4}$$

From Eq. (4), we deduce the kinematic model of the New SPM presented in Eq. (5):

$$\mathbf{B}\dot{\Theta} = \mathbf{A}\Omega \tag{5}$$

$\dot{\Theta}$ is the vector of the angular velocities of the active joints.

Matrix **A** represents a 4×3 matrix known as the parallel part of the Jacobian matrix, and Matrix **B** is a 4×4 diagonal matrix referred to as the serial part of the Jacobian matrix. Its expressions are as follows:
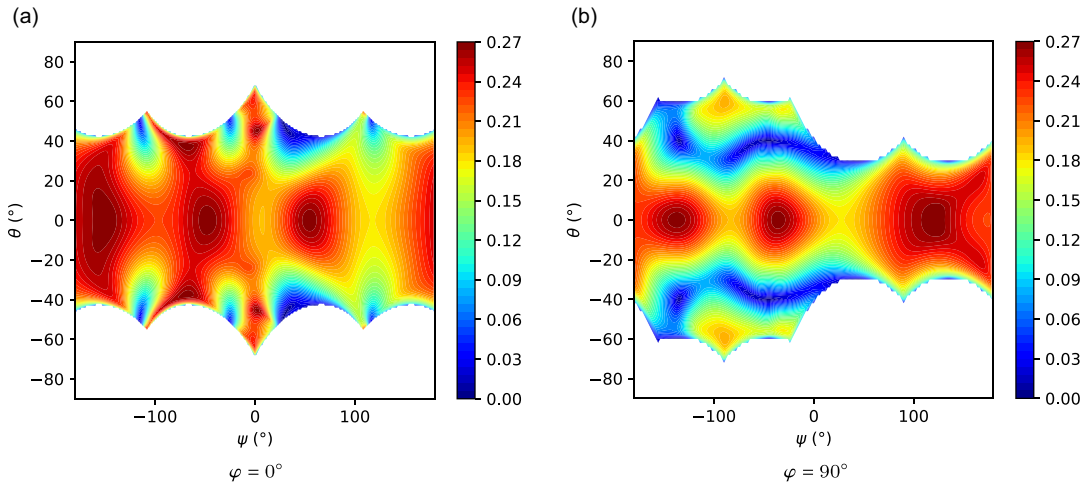
Figure 4. *Dexterity distribution for (α, β, δ, γ)=(50°, 50°, 55°, 15°).*

$$\mathbf{A} = \begin{bmatrix} (\mathbf{Z}_{2A} \times \mathbf{Z}_1)^T \\ (\mathbf{Z}_{2B} \times \mathbf{Z}_1)^T \\ (\mathbf{Z}_{2C} \times \mathbf{Z}_2)^T \\ (\mathbf{Z}_{2D} \times \mathbf{Z}_2)^T \end{bmatrix} \text{ and, } \mathbf{B} = \begin{bmatrix} \mathbf{Z}_{1A} \times \mathbf{Z}_{2A} \cdot \mathbf{Z}_1 & 0 & 0 & 0 \\ 0 & \mathbf{Z}_{1B} \times \mathbf{Z}_{2B} \cdot \mathbf{Z}_1 & 0 & 0 \\ 0 & 0 & \mathbf{Z}_{1C} \times \mathbf{Z}_{2C} \cdot \mathbf{Z}_2 & 0 \\ 0 & 0 & 0 & \mathbf{Z}_{1D} \times \mathbf{Z}_{2D} \cdot \mathbf{Z}_2 \end{bmatrix}$$

Since the New SPM is redundant, matrix $\mathbf{A}$ is not invertible. Consequently, we must calculate the inverse of the Jacobian matrix, rather than the Jacobian matrix itself. The inverse of the Jacobian matrix of the parallel manipulators is defined by:

$$\mathbf{J}^{-1} = \mathbf{B}^{-1}\mathbf{A} \tag{6}$$

Dexterity is an evaluation criterion, which indicates the ability of a robot to perform movements around a point in its workspace [25, 26]. Dexterity is often used to measure the efficiency with which a robot can reach a desired position while avoiding singular configurations. The expression of dexterity is as follows:

$$\eta(\mathbf{J}) = \frac{1}{\kappa(\mathbf{J})} \tag{7}$$

Where $\kappa(\mathbf{J})$ is the condition number of the Jacobian matrix, $\mathbf{J}$, given by $\kappa(\mathbf{J}) = \|\mathbf{J}\| \cdot \|\mathbf{J}^{-1}\|$.

When dexterity is equal to zero, the robot is in a singular configuration. For an arbitrary New SPM dimensions defined by $(\alpha, \beta, \delta, \gamma)=(50°, 50°, 55°, 15°)$, Fig. 4 shows that the dexterity is almost zero at the boundaries of the workspace for $\varphi = 0°$, and at some points within the workspace for $\varphi = 90°$, indicating the presence of parallel singularities. Although, as can be seen, the distribution of dexterity in the workspace is good, it is unfortunately low, not exceeding 0.27.

Figure 5 illustrates examples of parallel singularities occurring within the workspace. These singularities appear when the mobile platform and two branches of the same five-bar mechanism are aligned in the same plane. These singular positions are obtained for a New SPM with $\alpha_1 = \alpha_2 = 45°$, $\beta_1 = \beta_2 = 45°$, and $\gamma = 10°$. The cases (a) and (b) are in the working mode 7 and the case (c) is in the working mode 3 (see ref. [24]).

In the next section, we introduce an optimization approach for the New SPM. The main objective is to improve the dexterity of the New SPM and eliminate the singularities present in its workspace.
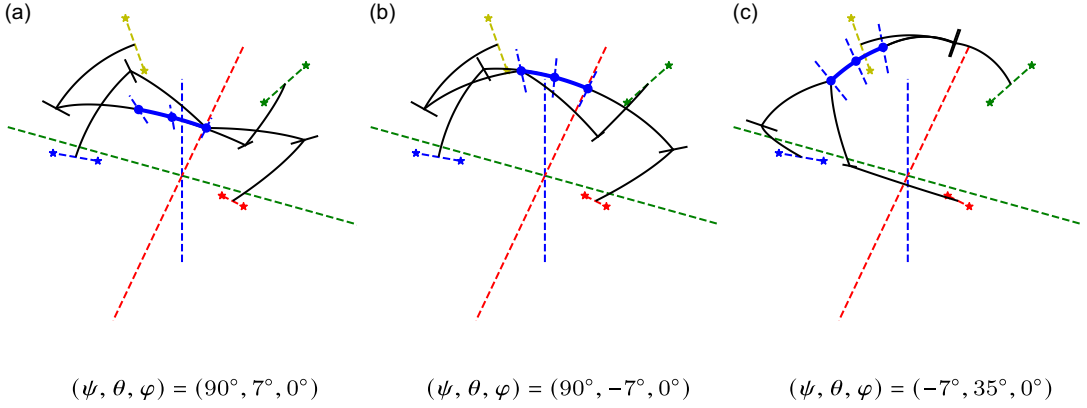
(a)   (b)   (c)

$(\psi, \theta, \varphi) = (90°, 7°, 0°)$ $(\psi, \theta, \varphi) = (90°, -7°, 0°)$ $(\psi, \theta, \varphi) = (-7°, 35°, 0°)$

Figure 5. *Some examples of singular positions for a New SPM with $\alpha_1 = \alpha_2 = 45°$, $\beta_1 = \beta_2 = 45°$, and $\gamma = 10°$.*

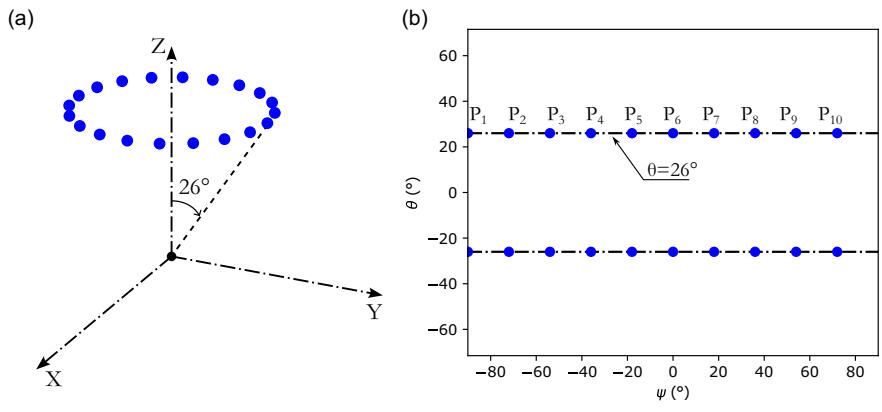**Figure 6.** *The prescribed workspace border (a) in Cartesian space (b) in (θ, ψ) plane.*

4. Optimization of the New SPM

Optimization consists of minimizing an objective function, which depends on parameters and is often subject to some constraints. To select the optimal geometric parameters for the New SPM, we employ optimization through genetic algorithms [27, 28]. The genetic algorithm is a stochastic search technique based on natural evolution. The genetic algorithm starts with an initial population of potential solutions (individuals), each representing a candidate solution to a problem. Over successive generations, genetic algorithms evaluate fitness, select individuals for reproduction, apply genetic operators (crossover and mutation), and create new offspring [29, 30]. The process continues until an ending criterion is met, resulting in the fittest individual known as the optimal solution. These methods are chosen due to their several advantages, including the simplicity of their mechanisms, ease of application, and efficiency even when dealing with complex problems.

The optimization aims to improve dexterity and cover the desired workspace. We define the desired workspace as a cone with a 26° apex angle. To make the optimization process easier, we only consider the workspace boundary in this work, as shown in Fig. 6.

Table I. *The lower and upper bounds of the geometric parameters for the first optimization.*

	α	β	γ
x_{inf}	40°	40°	5°
x_{sup}	80°	80°	25°
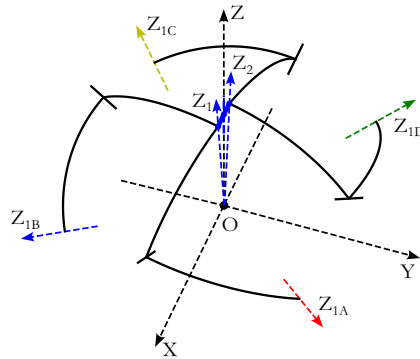
Figure 7. *Structure of New SPM resulting from the first optimization.*
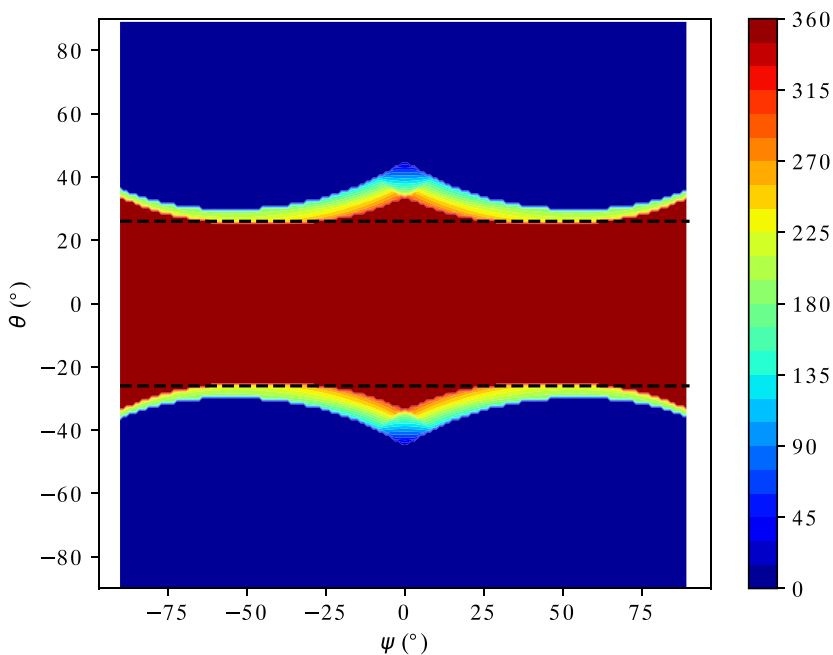
Figure 8. *Self-rotation distribution of the New SPM resulting from the first optimization.*

4.1. The first optimization

The first optimization aimed to minimize the geometric parameters in order to make the structure more compact, and ensure that the New SPM workspace covers the required workspace. In order to simplify the optimization procedure, a symmetrical structure is considered (where, $\alpha_1 = \alpha_2 = \alpha$ and $\beta_1 = \beta_2 = \beta$). We have optimized the geometric parameters defined by the design vector $\mathbf{X} = [\alpha, \beta, \gamma]$ and set $\delta = 70°$.

Figure 9. *Dexterity distribution of the New SPM resulting from the first optimization.*

Table II. *The lower and upper bounds of the geometric parameters for the second optimization.*

	α	β	γ
x_{inf}	40°	40°	10°
x_{sup}	80°	80°	25°

Figure 10. *Structure of New SPM resulting from the second optimization.*

The optimization process is formulated as follows:

$$\underset{X}{\text{minimize}} \quad F(\mathbf{X}) = \sum_{i=1}^{3} x_i^2$$

$$\text{Subject to} \quad x_i \in [x_{inf}, x_{sup}]$$

$$P_j \in WS(\mathbf{X}), j = 1..10$$

Where $F(\mathbf{X})$ represents the objective function, defined as the quadratic sum of the geometric parameters α, β, and γ. Minimizing $F(\mathbf{X})$ allows us to optimize the New SPM structure. x_{inf} and x_{sup} denote the lower and upper boundaries of the geometric parameters, as indicated in Table I.

To guarantee that all points P_j are in the workspace of the robot, the following condition is evaluated for each point P_j.

$$CD(\mathbf{X}, P_j) : \frac{C_i^2}{A_i^2 + B_i^2} \leq 1 \quad i = 1, .., 4 \text{ and } j = 1 \ldots 10 \tag{8}$$

The condition of Eq. (8) is evaluated for six different values of the self-rotation φ. These values are $\{0°, 60°, 120°, 180°, 240°, 300°\}$.

The genetic algorithm successfully converged to an optimal solution that meets the desired workspace and the constraints. The optimal structure is $(\alpha, \beta, \gamma) = (50°, 50°, 5°)$, which is presented in Fig. 7.

Figure 8 presents the capability of the New SPM to perform an unlimited self-rotation through its workspace. Thus, the optimal structure can achieve an unlimited self-rotation in the prescribed workspace.

The desired workspace is entirely contained within the New SPM workspace as shown in Fig. 9, which implies that the manipulator can achieve all the orientations required for the surgical tasks. However, the maximum dexterity value is below 0.1 for various values of self-rotation angle φ. This dexterity value is too low and shows the poor precision of the manipulator.

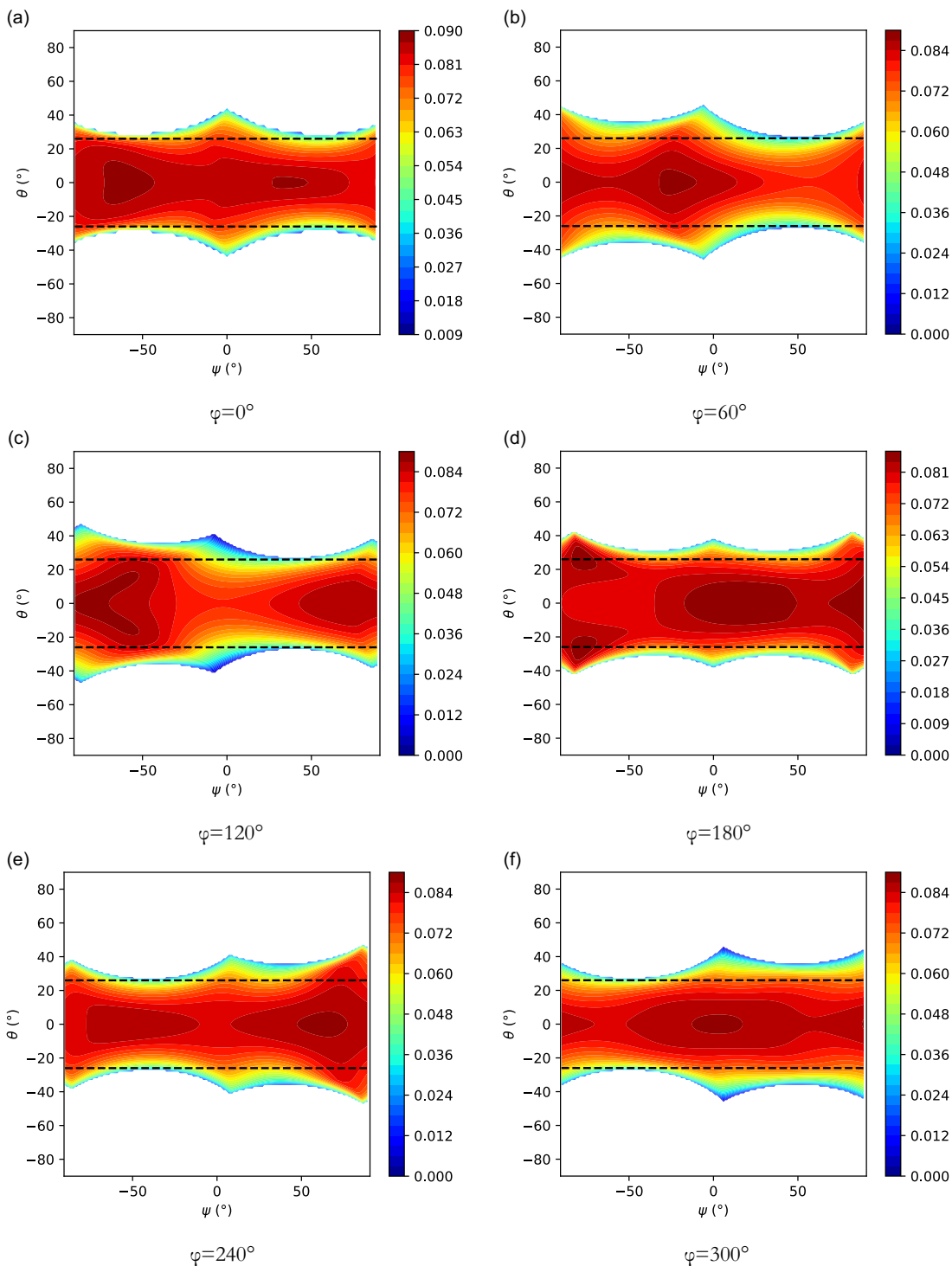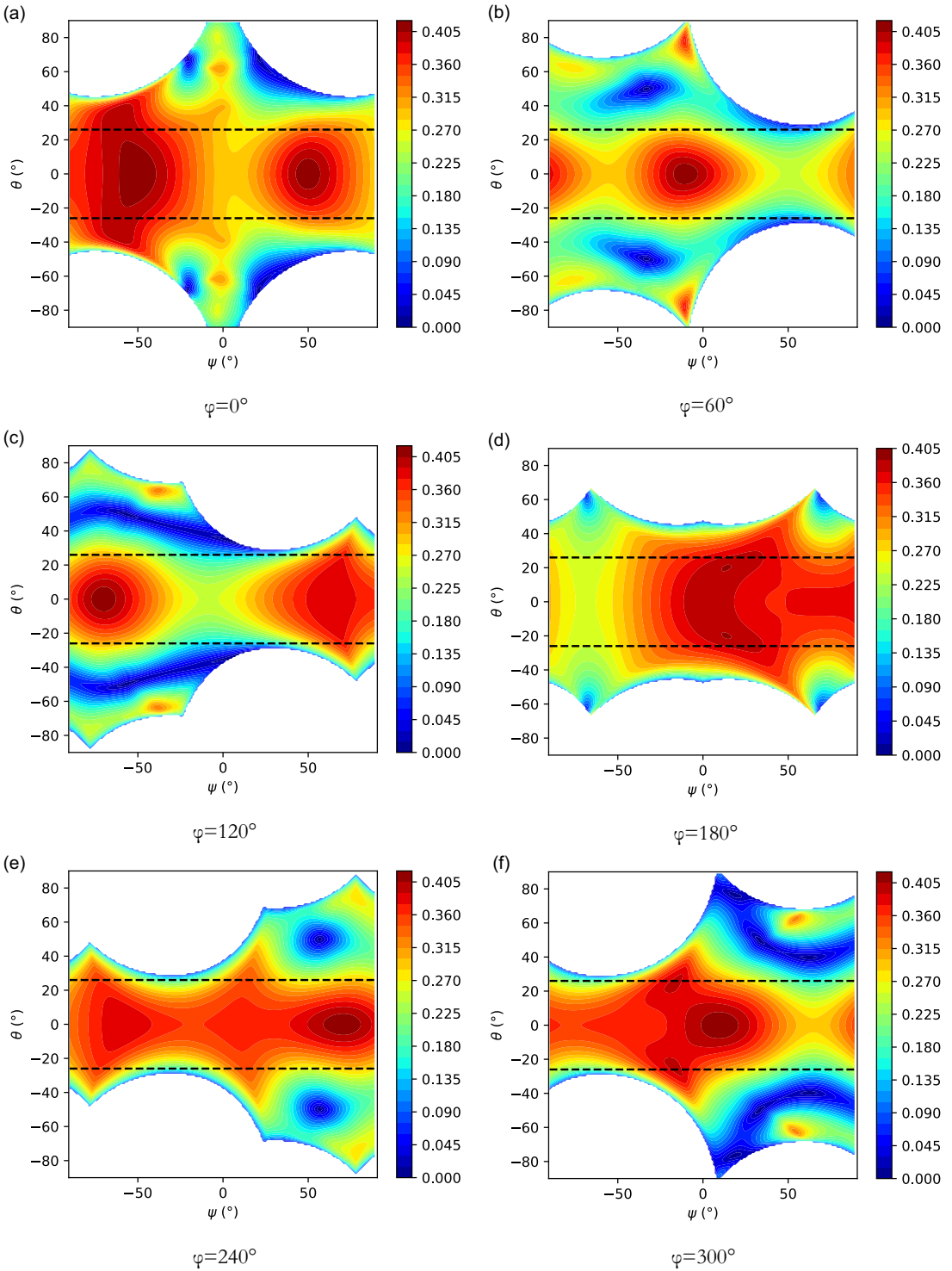**Figure 11.** *Dexterity distribution of the New SPM resulting from the second optimization.*
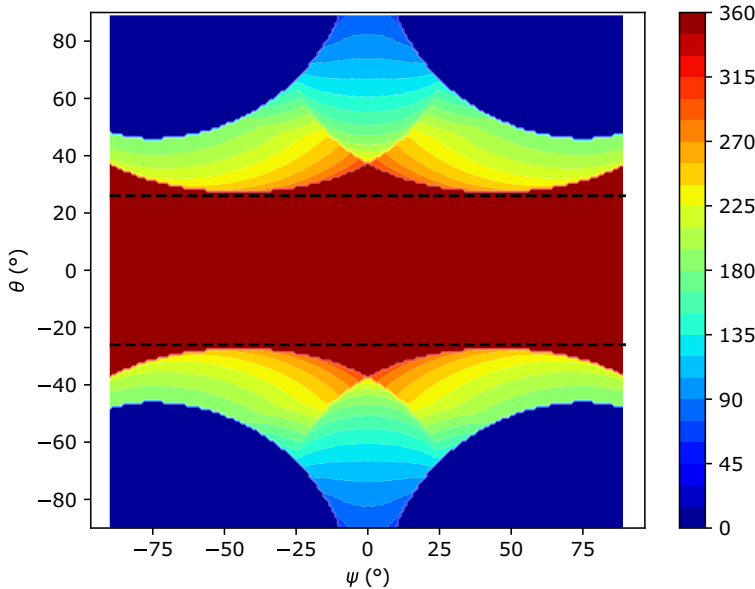
Figure 12. *Self-rotation distribution of the New SPM resulting from the second optimization.*

4.2. The second optimization

To enhance the dexterity, we will impose another constraint on the optimization process, related to the condition number such that:

$$CD(\mathbf{X}, P_j) : \kappa(\mathbf{J}) \leq \kappa_{\max} \quad j = 1 \ldots 10 \tag{9}$$

Where $\kappa_{\max}$ is the maximum acceptable value for the condition number, which is set to 25 (see, ref. [31]) during the optimization process.

As the first optimization, a symmetrical structure is considered. In addition, the same objective function is kept, while the lower limit of the angle γ is slightly modified, as indicated in Table II. This modification was necessary because a value of 5 for γ is quite minimal and gives a weak dexterity distribution.

Figure 10 presents the new optimal structure of the New SPM, where the optimal values of α, β, and γ are 60°, 60°, and 22.5°, respectively. We can easily see that the mobile platform angle γ has increased compared to the first optimization. Consequently, we can say that dexterity depends on the size of the mobile platform.

Figure 11 shows a good distribution of dexterity in the workspace for different values of φ, ranging from 0.3 to a maximum value of 0.4. This optimization resulted in a significant improvement compared to the result of the first optimization.

As shown in Fig. 12, the manipulator retains the ability to rotate 360° within the prescribed workspace.

In the two previous optimizations, the two five-bar mechanisms are considered symmetric. In order to investigate an asymmetric structure, a third optimization is carried-out in the next paragraph.

4.3. The third optimization

The third optimization was applied to an asymmetrical New SPM, where the parameters of the first five-bar are defined by α_1 and β_1, while the second mechanism is represented by α_2 and β_2. The new design vector is $\mathbf{X} = [\alpha_1, \beta_1, \alpha_2, \beta_2, \gamma]$.

Table III. *The lower and upper bounds of the geometric parameters for the third optimization.*

	α_1	β_1	α_2	β_2	γ
x_{inf}	40°	40°	40°	40°	10°
x_{sup}	80°	80°	80°	80°	25°
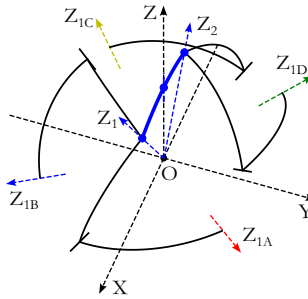
Figure 13. *Structure of New SPM resulting from the third optimization.*
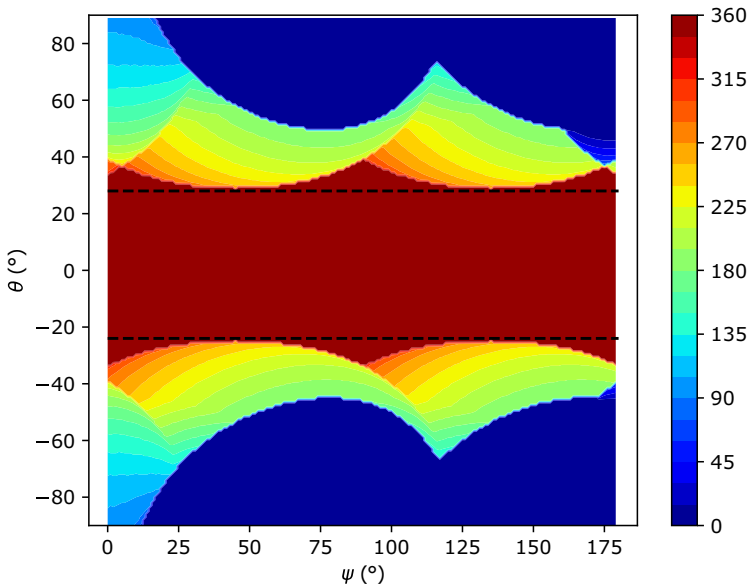
Figure 14. *Self-rotation distribution of the New SPM resulting from the third optimization.*

The same criteria were used as in the second optimization and the objective function is formulated as follows:

$$\underset{X}{\text{minimize}} \quad F(\mathbf{X}) = \sum_{i=1}^{5} x_i^2$$

$$\text{Subject to} \quad x_i \in [x_{inf}, x_{sup}]$$
$$P_j \in WS(\mathbf{X}), j = 1..10$$
$$\kappa(\mathbf{J}) \le \kappa_{max} \quad j = 1 \ldots 10$$

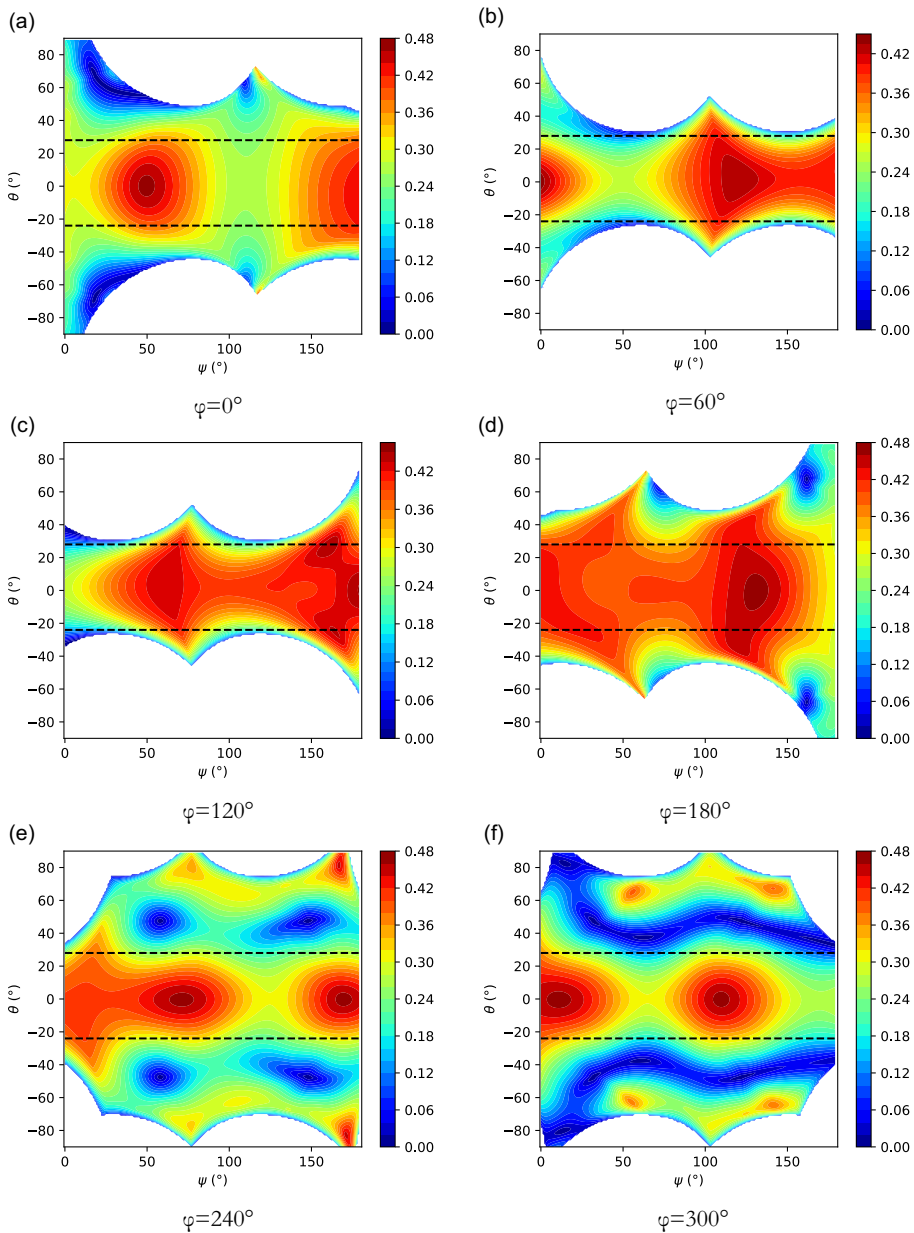The boundaries values x_{inf} and x_{sup} are defined in Table III.

Figure 15. *Dexterity distribution of the New SPM resulting from the third optimization.*

This New SPM optimization leads to the following vector of the design parameters :

$$\mathbf{X}_{op} = [\alpha_1, \beta_1, \alpha_2, \beta_2, \gamma] = [60°, 60°, 62°, 62°, 25°]$$

Figure 13 presents the optimal structure of the asymmetrical New SPM.

As shown in Fig. 14, the manipulator retains the ability to rotate 360° within the prescribed workspace. Due to the asymmetrical structure, the workspace distribution is slightly shifted, that is, it is not symmetrical with respect to zero.

This manipulator ensures a significantly improved distribution of dexterity across the workspace, with a higher maximum value than the previous optimization. Consequently, we achieve a reasonable
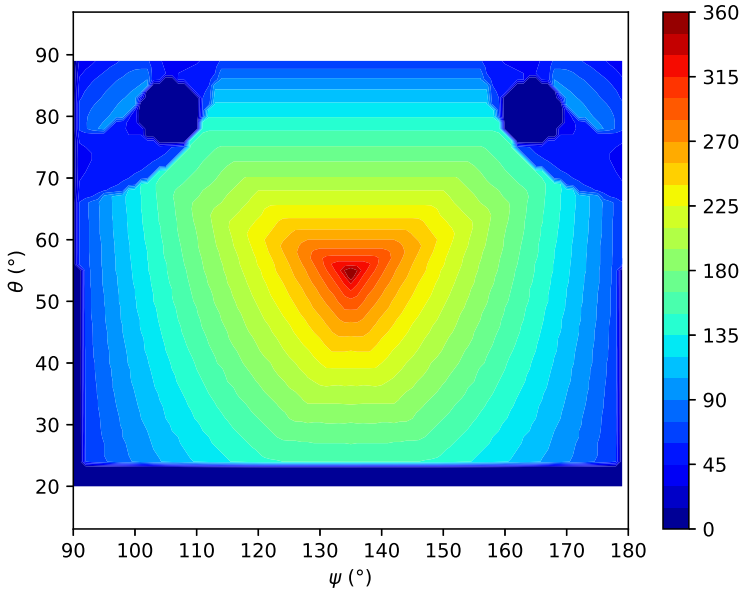
Figure 16. *Self-rotation capability in (°) of classical spherical parallel manipulator.*

dexterity distribution in the workspace, ranging from 0.3 to a maximum value of approximately 0.5. A good distribution of dexterity of the optimized manipulator is presented for different values of the self-rotation angle as shown in Fig. 15. It can be stated that dexterity is better in an asymmetrical system than in a symmetrical one. Indeed, the asymmetrical structure involves five parameters instead of three. The resulting values provide two different sets of α_1, β_1 and α_2, β_2, which leads to a better dexterity while maintaining the system's compactness.

For all the optimized structures obtained, we have always preserved the ability of the robot to perform unlimited self-rotation within the prescribed workspace.

As shown in Fig. 16, the self-rotation capability of the classical SPM [1] is highly limited. This approves the advantage of the proposed new parallel spherical manipulator over the classical SPM in terms of self-rotation.

As shown in the three optimizations, the dexterity depends on the size of the moving platform defined by the angle γ. When increasing γ, the dexterity index increases. In this work, an optimal structure is obtained by defining an optimization procedure. This structure has an acceptable dexterity distribution with a singular-free useful workspace. In addition, an unlimited self-rotation capability is guaranteed in this useful workspace.

In ref. [32], the forward kinematic model (FKM) is studied. The FKM of the proposed structure has a simple close-form solution. This is one of the advantages of the proposed kinematic. Future work will focus on the haptic control model of this redundant structure.

5. Conclusion

In this paper, a new redundant spherical parallel manipulator, called New SPM, has been developed. The New SPM consists of two five-bar mechanisms linked by a moving platform and provides three degrees of freedom. This new architecture offers unlimited self-rotation capability compared with the classical SPM. This work is aimed to improve the dexterity of the New SPM by applying three optimization procedures based on the genetic algorithm method. The first and the second optimizations were carried-out on a symmetric structure, while the third one was applied to an asymmetric structure. The first optimization resulted in a compact structure, while the second optimization of the New SPM resulted

in a notable improvement of the dexterity, which reached a value of 0.4. Finally, the third optimization of the asymmetrical structure resulted in a compact spherical parallel manipulator architecture while ensuring good dexterity with a maximum value of 0.48. In all three optimizations, an unlimited self-rotation capability is guaranteed in the useful workspace. In future work, a prototype will be made and experimentally validated. In addition, the proposed kinematics will be evaluated for tele-ultrasound application.

Author contributions. CL and HS conceived and designed the study. CL wrote the original draft. HS, AM, and MAL reviewed and edited the final manuscript. HS, AM, and MAL supervised the work.

Competing interest. The authors declare no conflicts of interest exist.

Ethical approval. Not applicable.

References

[1] A. Chaker, A. Mlika, M. A. Laribi, L. Romdhane and S. Zeghloul, "Synthesis of the spherical parallel manipulator for dexterous medical tasks," *Front. Mech. Eng.* **7**(2), 150–162 (2012).

[2] M. Meskini, H. Saafi, A. Mlika, M. Arsicault, S. Zeghloul and M. A. Laribi, "Development of a novel hybrid haptic (nHH) device with a remote center of rotation dedicated to laparoscopic surgery," *Robotica* **41**(10), 3175–3194 (2023).

[3] Y. Xie, X. Hou and S. Wang, "Design of a novel haptic joystick for the teleoperation of continuum-mechanism-based medical robots," *Robotics* **12**(2), 52 (2023).

[4] D. Escobar-Castillejos, J. Noguez, L. Neri, A. Magana and B. Benes, "A review of simulators with haptic devices for medical training," *J. Med. Syst.* **40**(4), 1–22 (2016).

[5] P. Garrec, J. P. Friconneau and F. Louveaux, "Virtuose 6D: A New Force-Control Master Arm Using Innovative Ball-Screw Actuators," **In:** *ISR 2004-35th International Symposium on Robotics* (2004).

[6] F. Najafi and N. Sepehri, "A novel hand controller for remote ultrasound imaging," *Mechatronics* **18**(10), 578–590 (2008).

[7] L. Birglen, C. Gosselin, N. Pouliot, B. Monsarrat and T. Laliberté, "SHaDe, a new 3-DOF haptic device," *IEEE Trans. Robot. Autom.* **18**(2), 166–175 (2002).

[8] Y. M. Han, S. B.Choi and J. S. Oh, "Tracking controls of torque and force of 4-degree-of-freedom haptic master featuring smart electrorheological fluid," *J. Intell. Mater. Syst. Struct.* **27**(7), 915–924 (2016).

[9] H. Khoshnoodi, A. Rahmani Hanzaki and H. A. Talebi, "Kinematics, singularity study and optimization of an innovative spherical parallel manipulator with large workspace," *J. Intell. Robot. Syst.* **92**(2), 309–321 (2018).

[10] H. Saafi, M. A.Laribi and S. Zeghloul, "Forward kinematic model resolution of a special spherical parallel manipulator: Comparison and real-time validation," *Robotics* **9**(3), 62 (2020).

[11] H. Saafi, M. A.Laribi and S. Zeghloul, "Optimal Haptic Control of a Redundant 3-RRR Spherical Parallel Manipulator," **In:** *2015 IEEE/RSJ International Conference on Intelligent Robots and Systems (IROS)* (IEEE, 2015) pp. 2591–2596.

[12] S. Leguay-Durand and C. Reboulet, "Optimal design of a redundant spherical parallel manipulator," *Robotica* **15**(4), 399–405 (1997).

[13] S. Bai, "Optimum design of spherical parallel manipulators for a prescribed workspace," *Mech. Mach. Theory* **45**(2), 200–211 (2010).

[14] G. F. Liu, Y. L. Wu, X. Z. Wu, Y. Y. Kuen and Z. X. Li, "Analysis and Control of Redundant Parallel Manipulators," **In:** *Proceedings 2001 ICRA. IEEE International Conference on Robotics and Automation (Cat. No. 01CH37164)* (IEEE), vol. **4** (2001) pp. 3748–3754.

[15] J. K. Arata, H.Kondo, N. Ikedo and H. Fujimoto, "Haptic device using a newly developed redundant parallel mechanism," *IEEE Trans. Robot.* **27**(2), 201–214 (2011).

[16] F. Marquet, O. Company, S. Krut and F. Pierrot, "Enhancing Parallel Robots Accuracy with Redundant Sensors," **In:** *Proceedings 2002 IEEE International Conference on Robotics and Automation (Cat. No. 02CH37292)* (IEEE), vol. **4** (2002) pp. 4114–4119.

[17] J. Wu, L. Wang and Z. You, "A new method for optimum design of parallel manipulator based on kinematics and dynamics," *Nonlinear Dyn.* **61**(4), 717–727 (2010).

[18] J. Wu, B. Zhang and L. Wang, "A measure for evaluation of maximum acceleration of redundant and nonredundant parallel manipulators," *J. Mech. Robot.* **8**(2), 021001 (2016).

[19] J. Wu, J. Wang, L. Wang and T. Li, "Dynamic formulation of redundant and nonredundant parallel manipulators for dynamic parameter identification," *Mechatronics* **19**(4), 586–590 (2009).

[20] J. Wang, J.WuT. Li and X. Liu, "Workspace and singularity analysis of a 3-DOF planar parallel manipulator with actuation redundancy," *Robotica* **27**(1), 51–57 (2009).

[21] H. Saafi, M. A. Laribi and S. Zeghloul, "Forward kinematic model improvement of a spherical parallel manipulator using an extra sensor," *Mech. Mach. Theory* **91**, 102–119 (2015).

[22] H. Saafi, M. A. Laribi and S. Zeghloul, "Redundantly actuated 3-RRR spherical parallel manipulator used as a haptic device: Improving dexterity and eliminating singularity," *Robotica* **33**(5), 1113–1130 (2015).

[23] I. Tursynbek and A. Shintemirov, "Infinite rotational motion generation and analysis of a spherical parallel manipulator with coaxial input axes," *Mechatronics* **78**, 102625 (2021).

[24] C. Lahdiri, H. Saafi and A. Mlika, "Working Mode Study of a New Spherical Parallel Manipulator with an Unlimited Self-Rotation Capability," **In:** *IFToMM International Conference on Mechanisms, Transmissions and Applications* (Cham, Springer Nature Switzerland, 2023) pp. 171–179.

[25] A. Hernansanz, J. Amat and A. Casals, "Optimization Criterion for Safety Task Transfer in Cooperative Robotics," **In:** *2009 International Conference on Advanced Robotics* (IEEE, 2009) pp. 1–6.

[26] J. Wu, J. Wang, T. Li, L. Wang and L. Guan, "Dynamic dexterity of a planar 2-DOF parallel manipulator in a hybrid machine tool," *Robotica* **26**(1), 93–98 (2008).

[27] M. A. Laribi, T. Essomba, S. Zeghloul and G. Poisson, "Optimal Synthesis of a New Spherical Parallel Mechanism for Application to Tele-Echography Chain," **In:** *International Design Engineering Technical Conferences and Computers and Information in Engineering Conference*, vol. **54839** (2011) pp. 579–587.

[28] J. Enferadi and R. Nikrooz, "The performance indices optimization of a symmetrical fully spherical parallel mechanism for dimensional synthesis," *J. Intell. Robot. Syst.* **90**(3-4), 305–321 (2018).

[29] S. Katoch, S. S. Chauhan and V. Kumar, "A review on genetic algorithm: Past, present, and future," *Multimed. Tools Appl.* **80**(5), 8091–8126 (2021).

[30] S. D. Stan, M.ManicR. Balan and V. Maties, "Genetic Algorithms for Workspace Optimization of Planar Medical Parallel Robot," **In:** *IEEE International Conference on Emerging Trends in Computing, ICETIC* (2009) pp. 8–10.

[31] H. Saafi, M. A. Laribi, M. Arsicault and S. Zeghloul, "Optimal Design of a New Spherical Parallel Manipulator," **In:** *2014 23rd International Conference on Robotics in Alpe-Adria-Danube Region (RAAD)* (IEEE, 2014) pp. 1–6.

[32] C. Lahdiri, H.Saafi, A. Mlika and M. A. Laribi, "Forward Kinematic Model Resolution of a New Spherical Parallel Manipulator," **In:** *The 8th International Symposium on Robotics and Mechatronics*, Djerba, Tunisia (2024).